Mechanical Properties and Reinforcement Mechanisms of Hydrogenated Acrylonitrile Butadiene Rubber Composites Containing Fibrillar Silicate Nanofibers and Short Aramid Microfibers

Ming Tian,[1,2] Lili Su,[2] Weiting Cai,[2] Shi Yin,[1] Qi Chen,[2,3] Hao Fong,[3] Liqun Zhang[1,2]

[1]*Key Laboratory of Carbon Fiber and Functional Polymers (Ministry of Education), Beijing University of Chemical Technology, Beijing 100029, China*
[2]*Key Laboratory of Beijing City on the Preparation and Processing of Novel Polymer Materials, Beijing University of Chemical Technology, Beijing 100029, China*
[3]*Department of Chemistry, South Dakota School of Mines and Technology, Rapid City, South Dakota 57701*

Received 19 February 2010; accepted 1 August 2010
DOI 10.1002/app.33121
Published online 29 November 2010 in Wiley Online Library (wileyonlinelibrary.com).

ABSTRACT: Short-fiber-reinforced rubber composites (SFRCs) with hydrogenated acrylonitrile butadiene rubber (HNBR) as the matrix and fibrillar silicate (FS) nanofibers and short aramid microfibers (DCAFs) as the fillers were developed, and their tensile properties, compression moduli, and mechanical anisotropies were investigated. The results indicated that the properties of the HNBR/DCAF/FS composites were determined by the loadings of the FS nanofibers and DCAF microfibers. A small amount of the microfibers combined with an appropriate amount of the nanofibers resulted in synergetic reinforcement and imparted to the SFRCs significantly improved mechanical properties without substantially compromising the rubbery characteristics. © 2010 Wiley Periodicals, Inc. J Appl Polym Sci 120: 1439–1447, 2011

Key words: clay; composites; fibers; mechanical properties; rubber

INTRODUCTION

Short-fiber-reinforced rubber composites (SFRCs) have attracted growing interest because they possess significantly improved mechanical properties but retain unique rubbery characteristics.[1,2] When they are impregnated with aligned fibers, SFRCs exhibit rigidity in the direction parallel to the fiber axes (the L direction) and viscoelasticity in the direction perpendicular to the fiber axes (the T direction); therefore, the mechanical properties of such SFRCs are anisotropic. For example, rubber composites reinforced with polyester or nylon short fibers are widely used in many commercial products, including the bottom rubber part of automobile drive belts, tire treads, tank track panels, seal components, vibration separators, and screen nets.[3–5] In addition to micrometer-scaled fibers (e.g., conventional microfibers of polyester and/or nylon), numerous nanofibers, including carbon nanotubes,[6–8] carbon nanofibers,[9–11] halloysite nanotubes,[12] and electrospun nanofibers,[13] have also been studied for the development of SFRCs. In comparison with microfibers, nanofibers are more likely to impart to SFRCs high mechanical and/or functional properties, controlled degrees of anisotropy, and desirable appearances.[2,14–17] Recently, considerable research has been devoted to investigating efficient methods for achieving uniform dispersions of nanofibers and to improving the interfacial properties of rubber matrices and nanofiber fillers.

Fibrillar silicates (FSs) are interesting naturally occurring clays containing magnesium and aluminum; the most abundant type of FS is known as attapulgite or palygorskite. The FS used in this study was attapulgite obtained from China, and its chemical formula is $Mg_5[Al]Si_8O_{20}(HO)_2(OH_2)_4{\cdot}4H_2O$. The FS structural units are single silicate crystals (nanofibers) that are 100–3000 nm long and 10–25 nm in diameter; these FS nanofibers agglomerate into micrometer-sized particles.[17–19] The FS nanofibers possess a high degree of structural perfection and superior mechanical properties. For example, the tensile strength of FS nanofibers has been estimated to be approximately 50 GPa,[17] which is more than

Correspondence to: H. Fong (hao.fong@sdsmt.edu) and L. Zhang (zhanglq@mail.buct.edu.cn)

Contract grant sponsor: High Technology Research program of the Ministry of Science and Technology in China; contract grant number: 2009AA03Z338.

Contract grant sponsor: Chang-Jiang Scholar program of the Ministry of Education in China; contract grant number: IRT0807.

10 times higher than the tensile strength of microfibers. Unlike layered silicates (e.g., montmorillonite), which are difficult to completely exfoliate into nanoscaled silicate layers and to uniformly distribute in rubber matrices, FS is relatively easy to separate into nanofibers and to distribute uniformly in rubber matrices, particularly if the repeating units of the rubber macromolecules are polar.[18] This is because the interaction between the nanofibers in FS particles/agglomerates is much weaker than the interaction between silicate layers in montmorillonite; therefore, even without the chemical substitution of metal ions with alkyl ammonium ions (a widely adopted method for the intercalation/exfoliation of montmorillonite for the preparation of nanocomposites), FS agglomerates/particles can be separated into nanofibers by simple dispersion in polar solvents such as water and/or ethanol and vigorous mechanical stirring afterward.[17–19] Because there are abundant silanol (Si—OH) groups on the surface of FS nanofibers and these groups can react readily with silane coupling agents such as γ-(methacryloxy)propyltrimethoxysilane (KH570), the interfacial bonding strength between the silanized FS nanofiber filler and the rubber matrix can be quite strong.[17–19] SFRCs containing FS nanofibers with distinctly improved mechanical properties have been developed from natural rubber, ethylene–propylene diene rubber, styrene–butadiene rubber, chloroprene rubber, and butyronitrile rubber.[2] In comparison with SFRCs containing conventional microfibers, SFRCs containing FS nanofibers exhibited similar stress–strain behaviors and anisotropic mechanical properties (when the FS nanofibers were aligned), and they also demonstrated higher heat resistance and better processing properties and product appearance.[2,19]

Hydrogenated acrylonitrile butadiene rubber (HNBR) is produced by the hydrogenation of carbon–carbon double bonds in acrylonitrile butadiene rubber (NBR). The hydrogenation degree typically ranges from 80 to 99%; thus, only a small number of carbon–carbon double bonds are in the molecular structure of HNBR. In comparison with NBR, HNBR possesses not only similar resistance to oil, wear, and low temperatures but also substantially enhanced resistance to heat and ozone; therefore, HNBR has been extensively used for applications in which both oil resistance and heat resistance are required.[20] Because the HNBR macromolecule has highly polar nitrile (—C≡N) groups, silane-modified FS nanofibers are relatively easy to uniformly disperse in the HNBR matrix.[18] In this study, HNBR/FS nanocomposites were prepared by the *in situ* modification of FS with a silane followed by the incorporation of the silane-modified FS nanofibers into HNBR through mechanical blending with a two-roll mill; subsequently, short aramid microfibers (DCAFs) were added to prepare HNBR/DCAF/FS composites. The hypothesis was that synergetic reinforcement could be achieved through the combination of nanometer- and micrometer-scaled fibers. To test the hypothesis, the effects of the amounts of the silane coupling agent, FS nanofibers, and DCAF microfibers on the tensile properties, compression moduli, and mechanical anisotropies of the resulting SFRCs were systematically investigated. The study revealed that a small amount of microfibers combined with an appropriate amount of nanofibers resulted in synergetic reinforcement and imparted to the prepared SFRCs significantly improved mechanical properties without substantially compromising the rubbery characteristics.

TABLE I
Compositions of the Composites

Hydrogenated butyronitrile rubber (phr)	100
Peroxide (phr)	3.5
Silane-modified FS (phr)	Various
Chopped aramid fibers (phr)	Various

EXPERIMENTAL

Materials

HNBR (Zetpol 2010L; acrylonitrile concentration = 36.2 wt %) was purchased from Zeon Co. (Tokyo, Japan). FS (1250 mesh) was obtained from Dalian Global Mineral Co. (Dalian, China). Chopped DCAFs (3 mm long and 12 μm in diameter) were produced by Teijin Co. (Osaka, Japan). The silane coupling agent KH570 [CH_2=C(CH_3)COO$CH_2CH_2CH_2$Si(OCH_3)$_3$] was provided by Shuguang Chemicals Co. (Nanjing, China). Other chemicals were purchased from Beijing Chemical Reagents Co. (Beijing, China).

Preparation of the composites

The as-received FS was first desiccated in an oven at 120°C for 2 h; subsequently, the *in situ* modification of FS with KH570 and the uniform dispersion of FS into HNBR were simultaneously carried out with a two-roll mill. The distance between the rolls (ca. 1.0–1.5 mm) was carefully adjusted to allow the HNBR to possess the optimal viscosity, whereas FS and KH570 were added to the rubber incrementally to ensure a good dispersion. The HNBR/FS composite was obtained after the processing of the materials at 150°C for 20 min on the mill. After the composite was naturally cooled to the ambient temperature, DCAF microfibers and vulcanizing agents were mixed into the composite; the compositions are shown in Table I. The loading level of each

individual ingredient was counted per hundred parts of rubber. The curing time was determined with an oscillating disc rheometer. The composite was then vulcanized on a platen press with 25 tons of pressure at 180°C. For the preparation of the test specimens, the vulcanized composites were punched out with a gauged die. The tensile test specimens were 2 mm thick, and the compression test specimens had a cylindrical shape, a height of 28 mm, and a diameter of 12.5 mm.

Tests and characterizations

Tensile and compression tests were carried out according to ASTM D 412 and ISO 7743-1989, respectively. Five tensile specimens and three compression specimens were prepared and tested, and average values and standard deviations were determined. The compression modulus at a low strain level (<6%) was derived from the stress–strain curves with a linear fitting method. A Cambridge S-250MK3 scanning electron microscope, which was purchased from Cambridge Co. (Cambridge, UK), was used to examine the fracture surfaces of the composites with the tested tensile specimens. Before the scanning electron microscopy (SEM) examination, the specimens were sputter-coated with gold to prevent charge accumulation. A Hitachi H-800-1 transmission electron microscope, which was purchased from Hitachi Ltd. (Tokyo, Japan), was used to examine the orientation of the FS nanofibers in the composites, and the transmission electron microscopy (TEM) specimens were prepared at −100°C with a Reichert-Jung Ultracut microtome manufactured in Leica Camera AG (Leitz, Germany) and mounted onto 200-mesh copper grids. The microtome was used in the L direction with respect to the orientation of the fibers.

RESULTS AND DISCUSSION

HNBR/FS composites

Effects of the KH570 amount

FS nanofibers have abundant silanol (Si—OH) groups on the surface.[17,21] The selection of a silane for surface-modifying FS is based on the rubber matrix and curing system. A silane with a vinyl group is preferred for rubber with carbon–carbon double bonds and a curing system containing peroxides.[18] The KH570 silane with methacryloxyl groups was thus used to surface-modify FS in this study. As shown in Figure 1, the presence of FS (with or without silane modifications) distinctly strengthened HNBR. In comparison with the composite reinforced with unmodified FS, the composites reinforced with KH570-modified FS had higher tensile strength but lower elongation at break, and the tensile strength increased with the KH570 amount increasing. When the amount of KH570 was 10 phr or higher, however, the tensile strength of the composite decreased; this was due to the plasticization effect of an excessive amount of silane. The optimal amount of KH570 was determined to be 6 phr for the composite with 40 phr FS. Although some unmodified FS could be separated into nanofibers, particularly in the polar rubber matrix with strong molecular interactions (e.g., HNBR), the surface silanization could facilitate the separation of FS into nanofibers and enhance the fiber–rubber interactions.[2,17,18] The fiber–rubber interface in an SFRC is known to play an important role in the determination of the stress-transfer efficiency. With an increase in the tensile strain, the FS nanofibers (particularly unmodified ones) could detach from the surrounding rubber, and this could lead to the fracture of the composites. After FS was silanized, the composites showed appreciably higher tensile stresses at high strain levels (>50%) versus low strain levels (<50%).

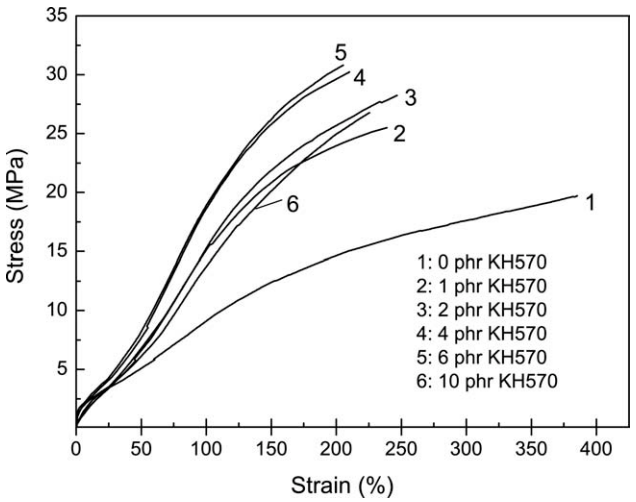

Figure 1 Tensile stress–strain curves of HNBR/FS composites filled with 40 phr FS modified with various amounts of KH570.

Effects of the FS amount

As shown in Figure 2, the pristine (unfilled) HNBR had low tensile stress and tensile strength, and the composites reinforced with KH570-modified FS had stress–strain characteristics similar to those of conventional SFRCs. These characteristics included high tensile stress with little deformation and low elongation at break. As the amount of KH570-modified FS was increased, the stress–strain curves of the composites became steeper. The critical loading of the modified FS was determined to be 40 phr. When the amount of FS was higher than 40 phr, the rate of change in the tensile stress of the composites

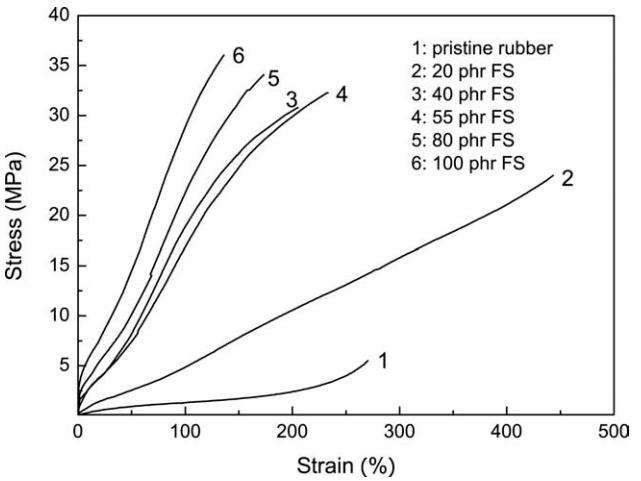

Figure 2 Tensile stress–strain curves of HNBR/FS composites filled with various amounts of KH570-modified FS.

decreased distinctly. When the FS amount exceeded 55 phr, the viscosity of the composites during processing became so high that mechanical mixing was difficult; this further hindered the complete separation of FS nanofibers from the particles/agglomerates. In general, the elongation at break decreased with the FS loading level increasing, but it still exceeded 100% even when the FS amount was 100 phr. Additionally, the compression moduli of the composites improved significantly with the FS loading level increasing (Fig. 3); the higher compression moduli indicated that the composites were more rigid, so a larger external force was required for similar compression deformation.

The orientation of the FS nanofibers in the composites was obtained with the nip gap between the rolls in the two-roll mill set to approximately 0.2 mm, which was much smaller than the gap of 1.0–1.5 mm during normal mixing processes; therefore, the shearing stress was substantially stronger, and anisotropic composites were then prepared. As reported by Fu and Lauke,[22] the fiber orientation had a significant impact on the tensile properties of the short-fiber-reinforced polymers. We used an indirect method of examining the orientation of short fibers: the ratios of the physical properties measured along the L and T directions were calculated. Such ratios of the mechanical properties measured along the L and T directions of the composites filled with various amounts of modified FS are shown in Figure 4. As the amount of KH570-modified FS was increased, the ratios of the tensile stresses at 25 and 100% strain levels as well as the ratios of the compression moduli in the L and T directions also increased. This indicated that the mechanical properties of the HNBR/FS composites were anisotropic. Such anisotropies were attributed to the orientation of the FS nanofibers induced by a mechanical shearing force. It is noteworthy that the composites showed mechanical anisotropies only when particles/agglomerates were well-separated into FS nanofibers. In comparison with conventional SFRCs containing microfibers, the composites containing nanofibers typically had a lower degree of fiber orientation. This was due to the fact that the short lengths and limited aspect ratios of the FS nanofibers allowed them to relax and/or rearrange after they were oriented during shearing, whereas the viscoelasticity of HNBR facilitated such relaxations and/or rearrangements. Consequently, the mechanical anisotropies of the HNBR/FS composites were not as high as those of conventional SFRCs containing aligned microfibers. For each HNBR/FS composite, however, the anisotropy of the tensile stress at 100% strain was higher than that at 25% strain because the elongation further aligned the

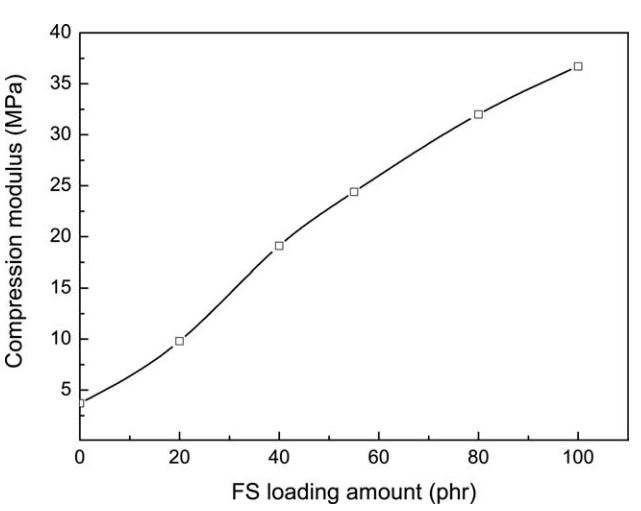

Figure 3 Compression moduli of HNBR/FS composites filled with various amounts of KH570-modified FS.

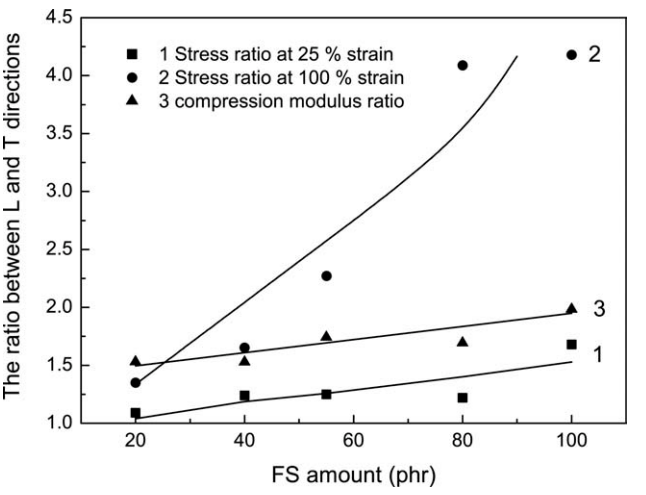

Figure 4 Ratios of the mechanical properties measured in the L and T directions to the fiber axes for HNBR/FS composites filled with various amounts of KH570-modified FS.

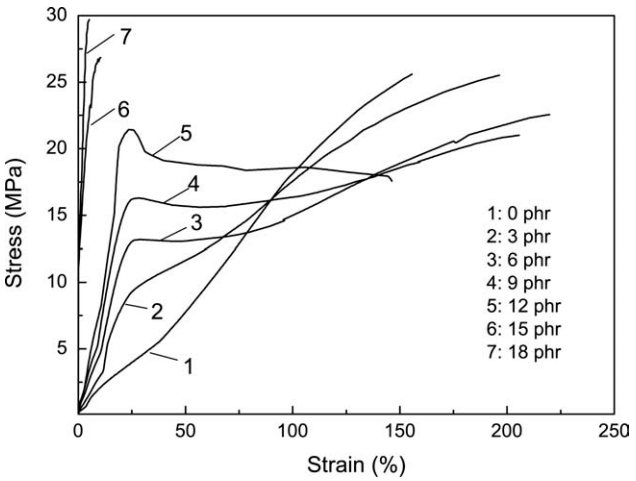

Figure 5 Tensile stress–strain curves (measured in the L direction) of HNBR/DCAF/FS composites filled with various amounts of DCAF microfibers (the FS amount was kept at 40 phr).

nanofibers. This was also the reason that the KH570-modified FS resulted in a greater increase in the tensile stress at a higher strain level.

HNBR/DCAF/FS composites

Effects of the amount of DCAF with the amount of FS kept at 40 phr

Although the HNBR/FS composites exhibited stress–strain characteristics and mechanical anisotropies similar to those of conventional SFRCs, the composites could be further reinforced through the incorporation of DCAF microfibers. As shown in Figure 5, the composites had a low tensile stress at low strain levels without DCAF, whereas the tensile stress was improved substantially by the incorporation of DCAF.

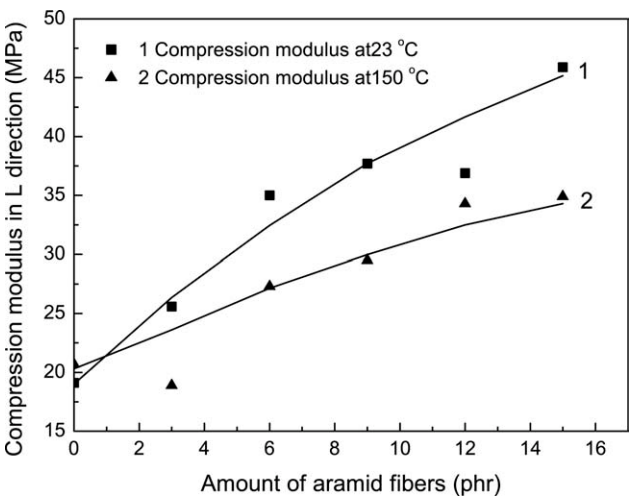

Figure 6 Compression moduli of HNBR/DCAF/FS composites filled with various amounts of DCAF microfibers at 23 and 150°C (the FS amount was kept at 40 phr).

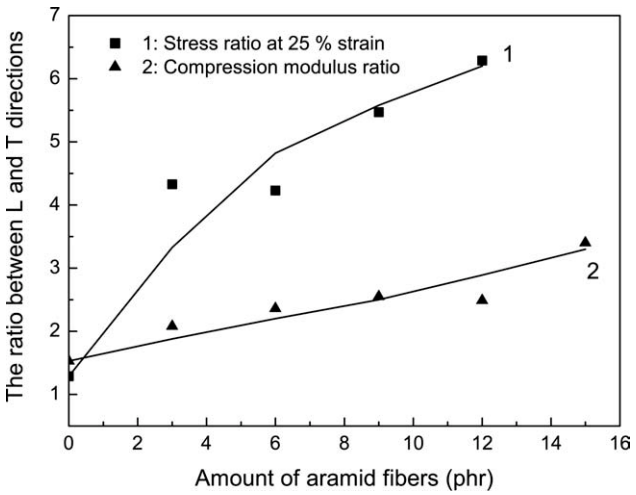

Figure 7 Anisotropies of compression moduli in the L and T directions for HNBR/DCAF/FS composites filled with various amounts of DCAF microfibers (measured at the strain level of 25% with the FS amount kept at 40 phr.

When the amount of DCAF was less than 12 phr, the composites demonstrated the tensile yield phenomenon (i.e., a plateau region in the curve) at 25% strain; this tensile yield was caused by the pullout of DCAF microfibers from the HNBR matrix due to the weak fiber–rubber interface. When the amount of DCAF was 15 or 18 phr, the stress–strain curves of the composites were much steeper, and the elongations at break were much lower; these composites no longer possessed the rubbery characteristic of large deformations, and it was also very difficult to fabricate the composites.

As shown in Figure 6, the compression moduli of the composites in the L direction increased with the amount of DCAF increasing whether the tests were conducted at the high temperature of 150°C or at room temperature (23°C). The compression modulus value measured at 150°C was lower than that measured at 23°C because, although the DCAF microfibers had excellent heat resistance, their modulus still decreased at a high temperature. As shown in Figure 7, the ratios of the compression moduli in the L and T directions for the HNBR/DCAF/FS composites, which were measured at the strain level of 25% with the FS amount kept at 40 phr, increased with the amount of DACF increasing. In comparison with those in Figure 4, the ratios in Figure 7 are higher, and this indicates that the composites were more anisotropic.

Effects of the FS amount with the amount of DCAF kept at 3 phr

The HNBR/DCAF/FS composites with a large amount of DCAF were hard to process; additionally, a uniform dispersion of DCAF microfibers was difficult to achieve, and the appearance of the composites was not desirable. Therefore, the composites containing low amounts of DCAF and reinforced with relatively

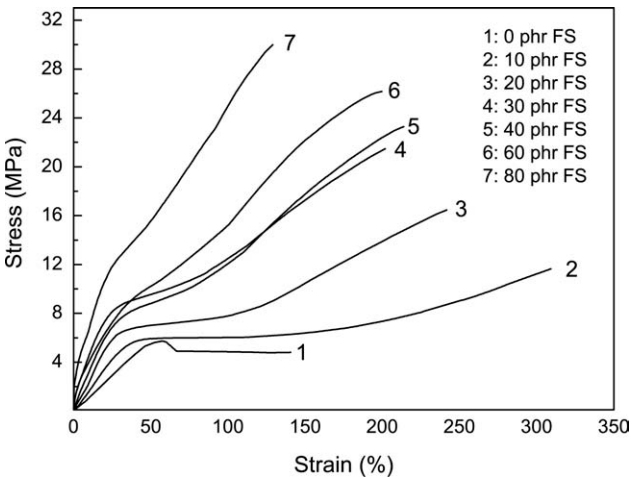

Figure 8 Tensile stress–strain curves (measured in the L direction) of HNBR/DCAF/FS composites filled with various amounts of KH570-modified FS and a small amount of DCAF microfibers (3 phr).

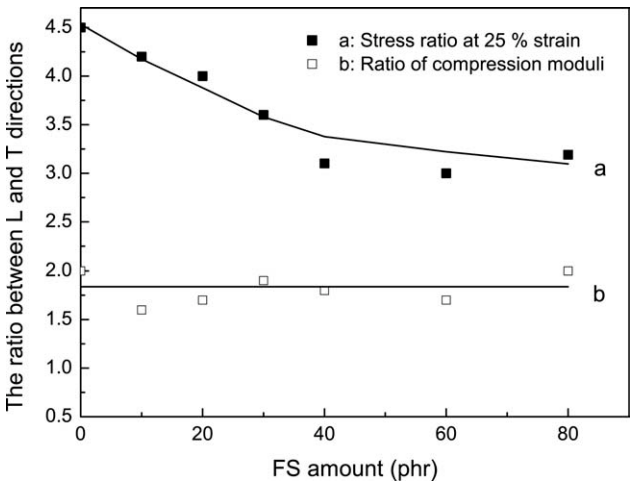

Figure 10 Anisotropies of stress at 25% strain and compression moduli of HNBR/DCAF/FS composites filled with various amounts of KH570-modified FS and a small amount of DCAF microfibers (3 phr).

large amounts of FS nanofibers had greater practical significance. Figure 8 shows the tensile stress–strain curves of the composites filled with various amounts of KH570-modified FS; the composites contained merely 3 phr of DCAF microfibers with an average length of 3 mm. It was evident that the tensile stress–strain curves of these composites had three distinctive stages: in stage 1, the tensile stress increased proportionally with the increase in the strain, and this was attributed to the short-fiber reinforcement through interface stress transfer at low strain levels (<50%); in stage 2, the tensile stress was kept almost constant because of the detachment of short fibers from the rubber matrix (termed the tensile yield); and in stage 3, the tensile stress increased continuously until the breaking of the rubber matrix occurred. The addition of FS improved the tensile stress–strain characteristics of the SFRCs. With an increase in the FS amount, the tensile stress increased slightly at low strain levels, and the tensile yield zone became narrower; finally, the tensile stress increased sharply until the composites were fractured. Consequently, the tensile strength of the composites increased, whereas the elongation at break decreased. It was concluded that the addition of FS effectively improved the tensile stress as well as the tensile strength at high strain levels (>50%) for the composites.

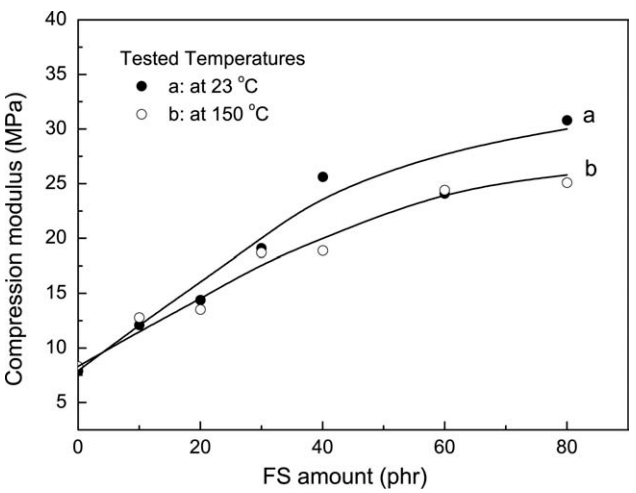

Figure 9 Compression moduli (in the L direction) of HNBR/DCAF/FS composites filled with various amounts of KH570-modified FS and a small amount of DCAF microfibers (3 phr) at 23 and 150°C.

Figure 9 shows that the compression moduli were improved with an increase in FS at both room temperature (23°C) and the high temperature of 150°C; nonetheless, the measured values of the compression moduli at different temperatures were almost identical. This indicated that the SFRCs had excellent compressive properties when they were reinforced with both FS nanofibers and a small amount of the DCAF microfibers. Figure 10 shows the anisotropies of stress at the 25% strain level and the compression moduli of the composites filled with various amounts of KH570-modified FS and a small amount of DCAF microfibers (3 phr). With an increase in the FS amount, the ratios of the tensile stress decreased slightly; the ratios of the compression moduli, however, remained almost the same. Collectively, the incorporation of a small amount of DCAF microfibers and various amounts of KH570-modified FS into the composites improved the tensile properties and the compression moduli and reduced the mechanical anisotropies.

Reinforcement mechanisms

Table II (corresponding to Fig. 5) shows the mechanical properties of the HNBR/DCAF/FS composites

TABLE II
Mechanical Properties of the HNBR/DCAF/FS Composites Filled with Various Amounts of DCAF Microfibers

Property / Direction	DCAF (phr) 0 L	0 T	3 L	3 T	6 L	6 T	9 L	9 T	12 L	12 T	15 L	15 T	18 L	18 T
Tensile stress at 5% strain (MPa)	1.1	0.9	1.5	0.7	2.6	1.1	3.3	1.3	4.1	1.4	22.3	2.6	29.6	2.8
Tensile stress at 25% strain (MPa)	3.6	2.8	9.1	2.1	13.1	3.1	17.5	3.2	21.4	3.4	–	5.6	–	6.5
Tensile strength at break (MPa)	25.3	22.4	25.5	17.3	22.8	17.6	21.0	16.5	18.2	14.7	28.2	15.1	29.6	14.7
Elongation at break (%)	157	213	197	279	220	230	206	241	137	254	12	197	5	176

The FS concentration was kept at 40 phr.

filled with various amounts of DCAF microfibers (the FS amount was kept constant at 40 phr). With an increase in the amount of DCAF microfibers, the tensile stress at a low strain was higher, the anisotropy of the tensile stress was larger, and the elongation at break was lower. Table III (corresponding to Fig. 8) shows the mechanical properties of the HNBR/DCAF/FS composites filled with various amounts of KH570-modified FS (the amount of DCAF microfibers was kept constant at 3 phr). With an increase in the amount of KH570-modified FS, the tensile stress at a low strain was also higher, and the anisotropy of tensile stress was also larger, but the impact on the tensile stress and the anisotropy at a low strain was far less than that of DCAF microfibers. It was evident that the increase in the FS amount also increased the tensile strength but decreased the elongation at break of the composites.

The SEM and TEM images in Figure 11 show the representative morphological structures of the HNBR/FS and HNBR/DCAF/FS composites with the amount of FS kept at 40 phr. The white spots in the images are the ends of FS nanofibers, which were roughly perpendicular to the fracture surface. It is noteworthy that FS was added before DCAF to HNBR to ensure that the FS particles/agglomerates could be well separated into nanofibers [Fig. 11(a)]. The SEM images indicate that most surfaces of the FS nanofibers had rubber remnants, and this suggests that the FS nanofibers were strongly bonded to HNBR and that the nanofiber–rubber interface was strong. When the DCAF microfibers were added to the composites, the uniform dispersion of FS nanofibers in HNBR was not distinctly affected [Figs. 11(b,c)]. The surfaces of DCAF, however, were smooth and did not have the attached rubber remnants; this suggests that the interfaces between the DCAF microfibers and the HNBR matrices were weak. This was further evidenced as follows: when the DCAF microfibers were detached (pulled out), holes were created on the fracture surfaces of the composites; these holes were roughly circular in shape and could weaken the composites as structural defects.

The stress-transfer theory could be adopted to explain the reinforcement mechanisms for SFRCs containing FS nanofibers and DCAF microfibers.[23] The mechanical properties of the SFRCs were primarily determined by the amounts and aspect ratios of the short fibers and the fiber–matrix interfacial adhesion.[22] The average length of the FS nanofibers was approximately 1 μm, and the aspect ratios were in the range of 10–30. Therefore, the FS nanofibers could not only support the matrix stress transfer but also prevent the propagation of microcracks in the matrix. In comparison with the FS nanofibers, the DCAF microfibers had a much larger aspect ratio of approximately 250; thus, they could bear higher loads at low strain levels and impart to the SFRCs higher degrees of mechanical anisotropy. With an increases in the tensile strain, the microfibers and the rubber matrices could detach, and the stress-transfer efficiency was determined by the interfacial adhesion. The microcracks could be initiated by the detachment of the DCAF microfibers from the HNBR matrices; and the DCAF microfibers were

TABLE III
Mechanical Properties of the HNBR/DCAF/FS Composites Filled with Various Amounts of KH570-Modified FS and a Small Amount of DCAF Microfibers (3 phr)

Property / Direction	FS (phr) 0 L	0 T	10 L	10 T	20 L	20 T	30 L	30 T	40 L	40 T	60 L	60 T	80 L	80 T
Tensile stress at 5% strain (MPa)	0.5	0.4	0.7	0.6	1.2	0.7	2.8	1.2	1.8	1.1	2.8	1.3	4.9	1.6
Tensile stress at 25% strain (MPa)	2.9	0.6	4.1	1.2	5.8	1.3	8.2	2	6.8	2.2	7.2	3	11.8	3.7
Tensile strength at break (MPa)	4.1	5.7	11.7	11.6	16.5	13.8	21.5	18.3	23.3	18	26.2	20.2	30	21.4
Elongation at break (%)	187	358	310	345	247	288	203	237	214	234	175	239	126	217

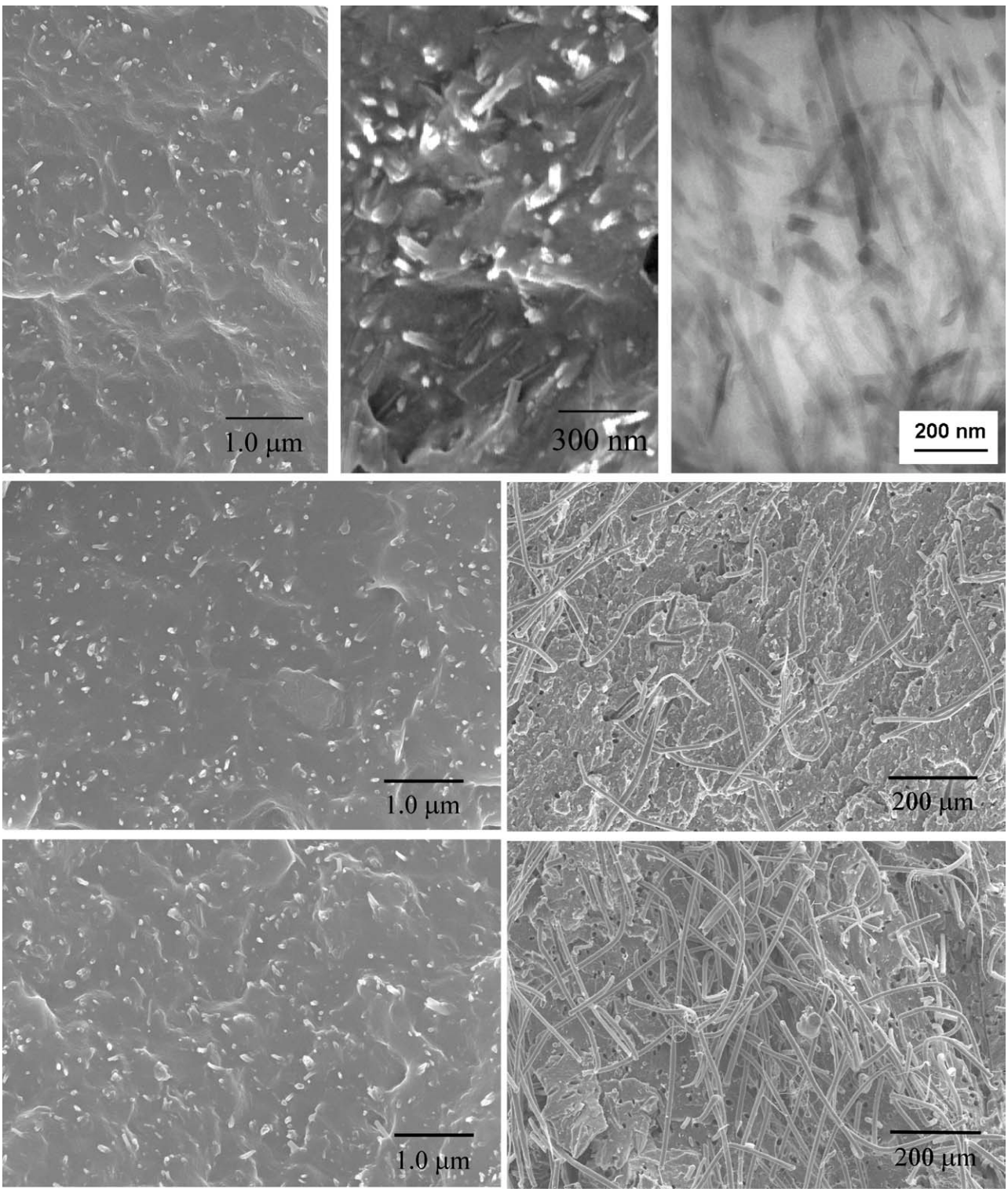

Figure 11 SEM and TEM micrographs of HNBR/FS and HNBR/DCAF/FS composites with various amounts of DCAF microfibers (the FS amount was kept at 40 phr): 0 (top), 3 (middle), and 15 phr DCAF (bottom).

much more likely to be pulled out from the rubber matrices than the FS nanofibers. As a result, DCAF made a more significant contribution to the tensile stress of the composites at low strain levels, whereas the FS nanofibers did at high strain levels; this led to higher tensile strength and elongation at break. In other words, when the composites reinforced by both DCAF microfibers and FS nanofibers were stretched, the microfibers first bore the loads transferred from the rubber matrices; when the strain levels were high, the nanofibers predominated in the role. It was suggested that when the load that DCAF

bore was much larger than that in the rubber matrix, the composites had lower elongation at break but higher tensile stress at low strain levels (e.g., the composites marked by curves 6 and 7 in Fig. 5). This situation is similar to that for conventional SFRCs. Otherwise, the composites had higher elongation at break and tensile strength (e.g., the composites marked with curves 2–4 in Fig. 5); this situation is typically found in nanocomposites with rubber matrices. When the load that DCAF bore was close to that in the rubber matrix, the composites showed tensile yields. In conclusion, the mechanical behaviors of the HNBR/DCAF/FS composites were determined by the loading levels of the DCAF microfibers and FS nanofibers. A small amount of microfibers combined with an appropriate amount of nanofibers could result in synergetic reinforcement and make the composites stronger and/or stiffer without the loss of the rubbery characteristics.

CONCLUSIONS

This study investigated the changes occurring in the structural and mechanical properties of HNBR composites when they were reinforced with FS nanofibers and DCAF microfibers. HNBR/FS nanocomposites were first prepared by the incorporation of KH570-modified FS into HNBR through a processing technique involving mechanical blending with a two-roll mill. DCAF microfibers were then added to develop the HNBR/DCAF/FS composites. The effects of the amounts of KH570, FS nanofibers, and DCAF microfibers on the tensile properties, compression moduli, and mechanical anisotropies of the composites were systematically investigated. The reinforcement mechanisms of FS nanofibers and DCAF microfibers were also analyzed. Because of the strong polarity of HNBR, the KH570-modified FS could be readily separated into nanofibers by the shearing force during the mechanical blending. The HNBR/DCAF/FS composites possessed mechanical anisotropies similar to the stress–strain characteristics of conventional SFRCs. DCAF microfibers made an important contribution to the tensile stress at low strain levels, whereas FS nanofibers made more of a contribution at high strain levels. The combination of an appropriate amount of FS nanofibers with a small amount of DCAF microfibers resulted in synergetic reinforcement and imparted to the composites significantly improved mechanical properties without substantially compromising the rubbery characteristics.

References

1. Murty, V. M.; De, S. K. J Appl Polym Sci 1984, 29, 1355.
2. Tian, M.; Lu, Y. L.; Liang, W. L.; Cheng, L. J.; Zhang, L. Q. Polym J 2006, 38, 1105.
3. Geethammaa, V. G.; Kalaprasad, G.; Groeninckx, G.; Thomas, S. Compos A 2005, 36, 1499.
4. Murty, V. M.; De, S. K. J Appl Polym Sci 1984, 29, 1355.
5. Rios, S.; Chicurel, R.; Castillo, L. F. Mater Des 2001, 22, 369.
6. Bokobza, L.; Kolodziej, M. Polym Int 2006, 55, 1090.
7. Bokobza, L.; Belin, C. J Appl Polym Sci 2007, 105, 2054.
8. De-Falco, A.; Goyanes, S.; Rubiolo, G. H.; Mondragon, I.; Marzocca, A. Appl Surf Sci 2007, 254, 262.
9. Kelarakis, A.; Yoon, K.; Sics, I.; Somani, R. H.; Hsiao, B. S.; Chu, B. Polymer 2005, 46, 5103.
10. Gauthier, C.; Chazeau, L.; Prasse, T.; Cavaille, J. Y. Compos Sci Technol 2005, 65, 335.
11. Karger-Kocsis, J.; Felhoes, D.; Thomann, R. J Appl Polym Sci 2008, 108, 724.
12. Du, M. L.; Guo, B. C.; Lei, Y. D.; Liu, M.; Jia, D. M. Polymer 2008, 49, 4871.
13. Kim, J. S.; Reneker, D. H. Polym Compos 1999, 20, 124.
14. Bhattacharyya, S.; Sinturel, C.; Bahloul, O.; Saboungi, M. L.; Thomas, S.; Salvetat, J. P. Carbon 2008, 46, 1037.
15. Das, A.; Stöckelhuber, K. W.; Jurk, R.; Saphiannikova, M.; Fritzsche, J.; Lorenz, H.; Klüppel, M.; Heinrich, G. Polymer 2008, 49, 5276.
16. Kita, T.; Hayashi, Y.; Wada, O.; Yanagi, H.; Kawai, Y.; Magario, A.; Noguchi, T. Jpn J Appl Phys Part 2 2006, 45, 1186.
17. Tian, M.; Liang, W. L.; Rao, G. Y.; Zhang, L. Q. Compos Sci Technol 2005, 65, 1129.
18. Tian, M.; Cheng, L. J.; Zhang, L. Q. J Appl Polym Sci 2008, 110, 262.
19. Tian, M.; Cheng, L. J.; Liang, W. L.; Zhang, L. Q. Macromol Mater Eng 2005, 290, 681.
20. Keller, R. W.; Klingender, R. C. Handbook of Specialty Elastomers; CRC: Boca Raton, FL, 2008; p 93.
21. Serna, C. J.; Vanscoyoc, G. E.; Ahlrichs, J. L. Am Mineral 1977, 62, 784.
22. Fu, S. Y.; Lauke, B. Compos Sci Technol 1996, 56, 1179.
23. Zhu, D. S.; Gu, B. Q.; Chen, Y. J Comput Theor Nanosci 2008, 5, 1546.